JOURNAL OF MATERIALS SCIENCE 28 (1993) 3617–3625

Mechanistic analysis of fatigue crack initiation in medium-density polyethylene

E. SHOWAIB, A. MOET
Department of Macromolecular Science, Case Western Reserve University, Cleveland, OH 44106, USA

Kinetics parameters of craze evolution preceding fatigue crack initiation (FCI) in medium-density polyethylene (MDPE) pipe materials were determined and analysed within fracture mechanics theory. A single craze initially preceded the notch tip, a root craze, which subsequently became accompanied by a few side crazes. Crack initiation transpired after the craze-zone growth had reached its fully developed configuration. The length of the root craze of the fully developed zone was found to be equal to the length of the first discontinuous crack band on the fracture surface. The growth of the root-craze length and the crack-tip opening displacement (CTOD) followed a power law over the major portion (94%) of the FCI time. Measurable rupture of the craze material was only noted within the final portion of the FCI time and was associated with exponential increase of the CTOD. The Dugdale/Barenblatt model overestimated the craze length by 30% and underestimated the CTOD by 50% which was hypothesized to be due to multiple crazing at the notch tip.

1. Introduction

Medium-density polyethylene (MDPE) copolymerized with other olefins are becoming an important class of materials for applications demanding long-term resistance to slow crack growth such as fuel gas pipes. Service lifetime in such applications is limited by the time to propagate a slow crack from a stress-concentration site. This limiting process comprises two components: time for crack initiation and time for stable (subcritical) crack propagation. Accelerated slow crack growth (SCG) testing of MDPE pipes under fatigue [1] and under constant load testing [2] indicates that crack initiation consumes about half the entire lifetime. However, theories of lifetime prediction [3, 4] consider crack propagation as the sole determining process limiting the useful service life. Overlooking the crack initiation stage in testing and in lifetime prediction stems from the scarcity of theoretical formulations for the problem of crack initiation, i.e. kinetics of damage processes leading to crack initiation from a stress concentrator of defined geometry. Evidently, crack initiation parameters such as K_{IC} and J_{IC} are of no use in lifetime prediction. The majority of theoretical developments dealing with crack initiation present mathematical relationships based on the accumulation of dislocations [5, 6], equivalent strain-energy density method [7, 8], and notch-tip local strain [8, 9] which are not amenable to experimental verification. Measurements on carbon steel [10] and polycarbonate [11] indicate that the local strain at the notch tip evolves to a set value at which crack initiation occurs. On a logarithmic scale the cumulative local strain was noted to be linear with the number of cycles of initiation at various fatigue loading conditions. The crack-tip opening displacement, is an affiliated parameter which is related to the stress field through appropriate fracture mechanics expressions. Measurements conducted on a polyethylene homopolymer at constant loads [12, 13] show that the CTOD evolves with time exponentially to a constant value of 25–30 μm for all stresses and notch depths. This observation suggests the CTOD to be a candidate parameter to quantify damage processes preceding crack initiation. However, the fact that multiple crazes are commonly observed to precede cracks in medium density ethylene copolymers [14, 15] limits the usefulness of the CTOD as a reliable measure of damage preceding the onset of crack initiation in this type of materials. It is also recognized that the accuracy of the predictions of crack initiation depends on the definition of the crack initiation [8].

The foregoing brief indicates the necessity for a thorough examination of the irreversible deformation processes preceding crack initiation in ethylene copolymers to construct the knowledge base required to develop a predictive formalism for the initiation stage of service lifetime. In the present work, detailed mechanistic investigation of the damage process preceding crack initiation was conducted in conjunction with kinetic measurements of craze growth and crack-tip opening displacement. The data have been analysed within a framework of fracture mechanics to define discerning crack-initiation criterion. In a subsequent publication, we employ the crack layer concept to formulate the problem.

2. Experimental procedure

Three MDPE pipe samples were provided by Osaka Gas Company, Japan. These are an ethylene–hexene

0022–2461

TABLE I The key difference in the chemical and physical properties of the three resins

Material		MFR (21.6 kg-g/10 min)	Average molecular weight		Molecular weight distribution	Type of branch
Composition	Symbol		M_W ($\times 10^4$)	M_N ($\times 10^4$)		
Ethylene–methyl-pentene copolymer	MP	0.21	14.0	2.1	6.6	Isobutyl
Ethylene–butene copolymer	B	0.21	15.0	1.2	12.5	Ethyl
Ethylene–hexene copolymer	H	0.20	12.0	1.3	9.5	Butyl

copolymer (H), an ethylene–methylpentene copolymer (MP), and an ethylene–butene copolymer (B). The material provided was in the form of an extruded gas pipe with 8.75 mm minimum wall thickness and average outside diameter of 89 mm. Table I illustrates the key difference between these resins [16, 17]. The fatigue-test specimen was an arc segment of a pipe ring with a 28 mm width shown in Fig. 1, which is similar to the C-shaped geometry described in ASTM E-399 [18]. The distance between loading holes is 21 mm centre-to-centre. This distance is selected to avoid reverse bending associated with relatively long cracks. The holes were reinforced by steel sleeves to minimize frictional effects. A fresh razor blade was used for each specimen to introduce a 2.0 mm $\pm$ 1% deep notch in the hoop direction, with an insertion speed of 0.05 mm min^{-1} [19]. The razor blade had an equal angle double-ground head supplied from O.E.C. Company, Medina, OH. Maintaining the quality of the edge of the razor blade is necessary to achieve reproducible crack-initiation results. To avoid discrepancies due to residual stress effects, each specimen was tested after a period of 15 days, elapsed from the time it was cut from the pipe [1].

An MTS servohydraulic machine was used to apply a sinusoidal load form at a constant frequency (0.5 Hz) on the test specimen. The test was performed under tension–tension (T–T) fatigue loading with a minimum to maximum load ratio, R, equal to 0.1. The maximum load was set to produce a stress of 6.00 MPa calculated by dividing the force by the cross-sectional area. This level of stress is about 30% of the yield stress of the materials (Table II). A travelling optical microscope attached to a video camera was used to observe the crack/craze front during the test. Thin sections were cryogenically prepared from the mid-plane of the specimen to examine the craze microstructure using optical microscopy. In this examination, a section was attached to a microscope slide using adhesive tape in such a way as to induce a crack-opening profile close to that experienced by the specimen under fatigue loading. Scanning electron microscopy was employed to examine the fracture surface.

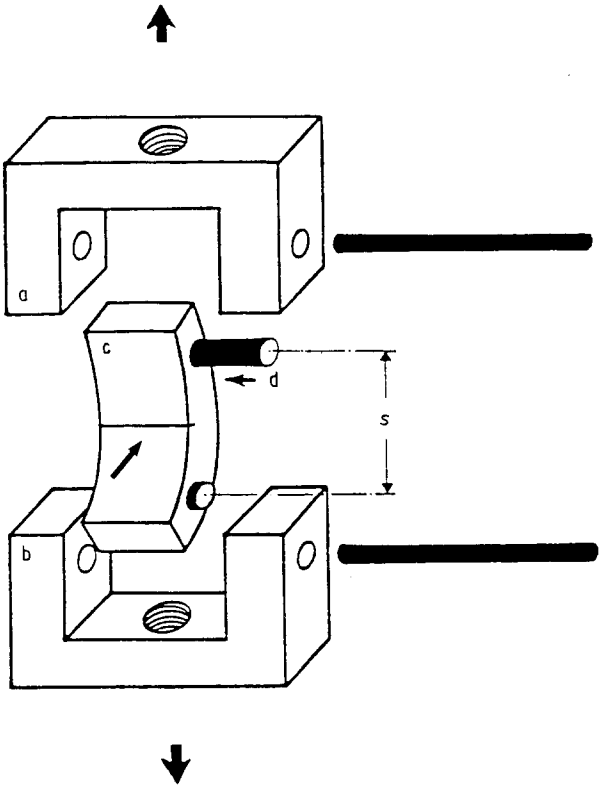

Figure 1 Schematic drawing showing gripping fixtures, a, b, test specimen, c, reinforcing sleeves, d, and distance, s, between loading holes.

3. Results

Fig. 2 is a micrograph of a portion of the left half of the fracture surface showing the typical stages of FCP in MDPE copolymers. The discontinuous crack-growth bands start from the notch. The first band comprises the crack-initiation region, followed by three other bands indicative of brittle crack growth and finally ductile fracture. Typically, the boundary of the band, which demarcates the crack-arrest line, displays a curvature due to increased plane-stress contribution towards the edges of the specimen. This paper deals primarily with detailed analysis of the processes contributing to crack advance into the first band (Fig. 2), i.e. crack initiation. The analysis of crack initiation is driven by several fundamental factors.

First, total fatigue lifetime, N_t (Table III), correlates very well with the number of cycles for crack initiation, N_i, as well as with the number of cycles for brittle crack propagation. Some polyethylene (PE) materials, for example butene copolymer (B), exhibit dispropor-

TABLE II Mechanical properties of the three copolymers using ASTM D1708-84

Material	E (MPa)	σ_y (MPa)	σ_{ut} (MPa)	ε_{ut} (%)
MP	405	19.7	22.1	890
B	376	19.7	22.1	890
H	387	18.8	19.6	805

TABLE III Comparison of lifetime data in the three copolymers; N_i is the number of cycles of initiation, N_b the number of cycles of brittle propagation, N_d the number of cycles of ductile failure, and N_t the total number of cycles. Reprinted from [1].

Material	N_i ($\times 10^3$)	N_b ($\times 10^3$)	N_d ($\times 10^3$)	N_t ($\times 10^3$)
MP	158.0	184.4	9.3	378.3
B	110.2	130.2	88.3	328.7
H	47.3	37.3	3.7	88.3

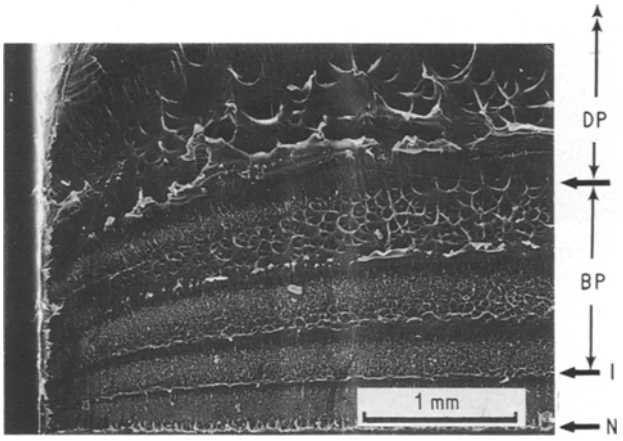

Figure 2 Scanning electron micrograph of a portion of the left half of the fracture surface, where N is the notch, I is the initiation, BP is the brittle propagation, and DP is the ductile propagation.

tionate (long time) ductile crack-propagation resistance which is of no concern in assessing long-term performance in service. The latter is determined by the resistance of the material to brittle crack propagation [20, 21]. The second factor stems from the fact that crack initiation is the first step into brittle crack propagation. Examination of the fracture surface in Fig. 2 indicates that the first band (crack initiation) is more brittle, i.e. flatter (slit-like) than subsequent crack excursions. The third factor originates from the scarcity of studies dealing with crack initiation in general.

A microscopic view into the root of the notch (Fig. 3) reveals a whitened strip, AA′, bounded by optical reflections of the notch boundaries BB′. The whitened strip AA′ is the reflection of the craze membrane, constituting the notch/craze interface. Thus, the span AA′ represents the crack-tip opening displacement (CTOD). The craze membrane has an elliptical appearance at both ends (only one is shown in Fig. 3). During fatigue loading, this membrane is being continuously viewed by the optical microscope to observe changes in CTOD and the associated damage evolution.

The CTOD measured at the centre of the craze membrane as a function of loading cycles is shown in Fig. 4. A rapid increase from 4 μm to about 150 μm is observed to have occurred within the first 20 000 cycles (15% N_i). The value of the CTOD remains constant for the next 100 000 cycles, and starts to take off at 125 000 cycles (arrow R, Fig. 4). An exponential rise in the CTOD leads to crack initiation at 133 000 cycles (arrow I). After initiation, the same pattern appeared to be repeated as FCP continues.

To follow the rate of craze growth associated with the noted evolution in CTOD, a series of identical tests were conducted under identical conditions, then were interrupted at selected intervals of fatigue cycles. The specimens were then unloaded and thin sections were prepared at the mid-plane of each specimen, and examined in transmitted light microscopy. Plane-stress effects at both sides of the specimen inhibited direct craze appearance. That is why craze growth has to be viewed from mid-plane sections. The results are displayed in Fig. 5.

As a result of inserting the razor blade into the specimen, prior to fatigue loading, a 20 μm root craze develops at the notch tip. The craze shown in the top micrograph of Fig. 5 is that of a craze in a specimen after experiencing a single loading cycle. The craze length here is 270 μm which is about 14 times its preloading length. At 500 cycles, the root craze grew slightly and two sets of side crazes emanate from the notch tip at an angle of about 23°. The root crazes became larger and wider, as did the side crazes. The configuration of crack-tip plasticity shown in Fig. 5, which is composed of a root craze flanked by two or more side crazes, is commonly reported for several medium-density PE copolymers [14, 15, 21]. The craze-growth data shown in Figs 5 and 6 were generated from MP copolymer. The two other copolymers exhibit similar behaviour.

A plot of the craze length as a function of the number of cycles in MP copolymer is shown in Fig. 6. A close similarity is noted between the craze-growth behaviour and that of the CTOD (Fig. 4). A comparison between Figs 2 and 5 indicates that the craze length at 70 000 cycles ($\sim$ 0.6 mm) is close to the length of the first band ($\sim$ 0.5 mm). Noting that crack initiation occurred at 133 000 cycles, one may conclude that the craze at 70 000 cycles might have maintained its configuration during the remaining number of cycles, during which damage of the craze material progressed leading to its rupture (cracking). Indeed, viewing the front craze membrane indicated that the onset of visible rupture was only observed at 125 000 cycles (arrow R, Fig. 4). Significant damage of the craze material probably occurred between the onset of the exponential increase in the CTOD and crack initiation (arrow I, Fig. 4). Even though the craze-material damage could occur within the entire craze, its magnitude is directly accessible by observing rupture in the front membrane.

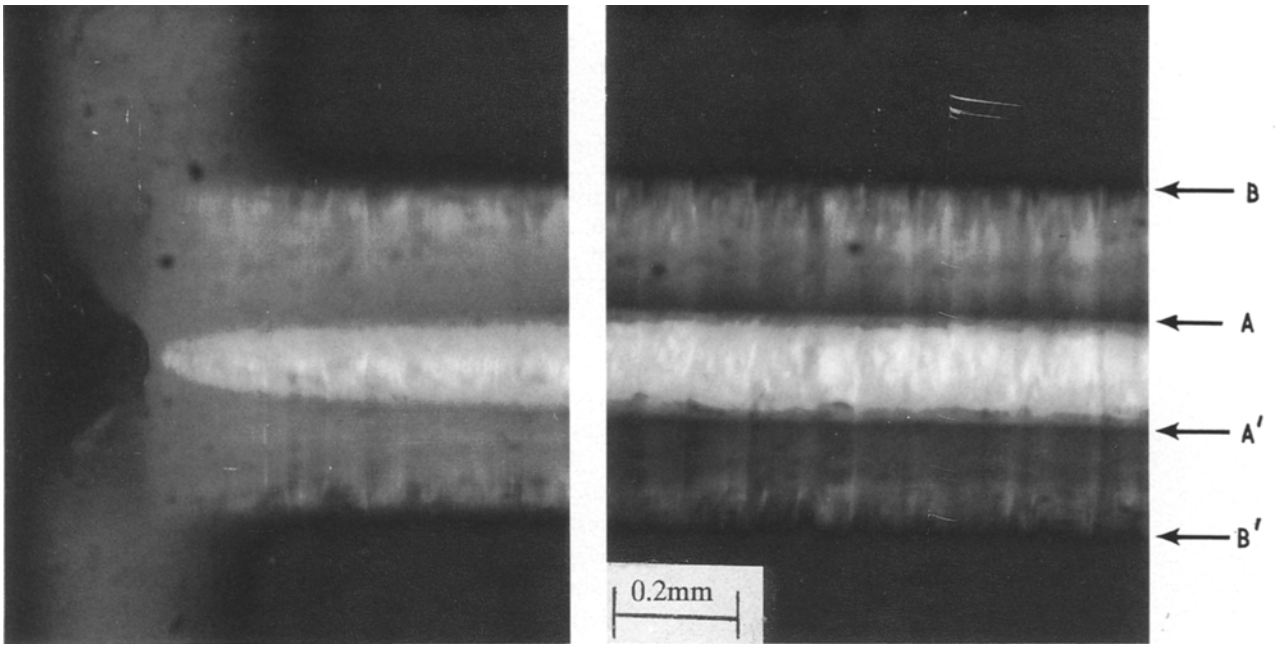

Figure 3 Microscope views into the root of the notch showing the craze front AA′ and the notch opening BB′. The photograph on the right shows the centre of the craze front, while the photograph on the left shows the effect of plane stress at the left edge of the specimen.

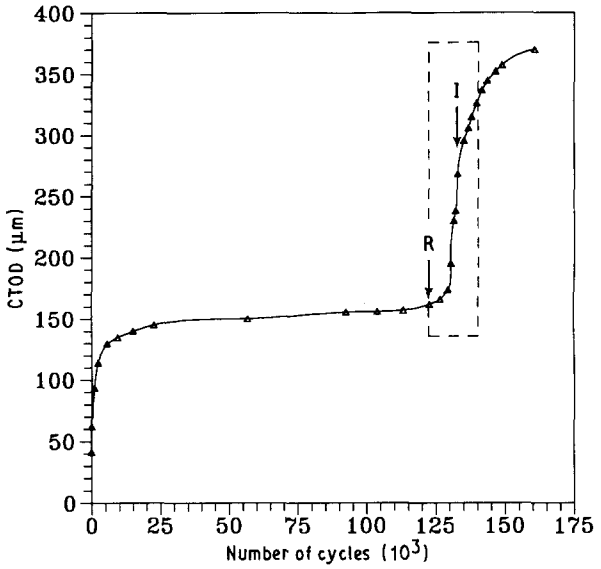

Figure 4 The CTOD history measured at the centre of the craze membrane. I indicates the designated initiation point, and R indicates the point at which the curve starts to take off.

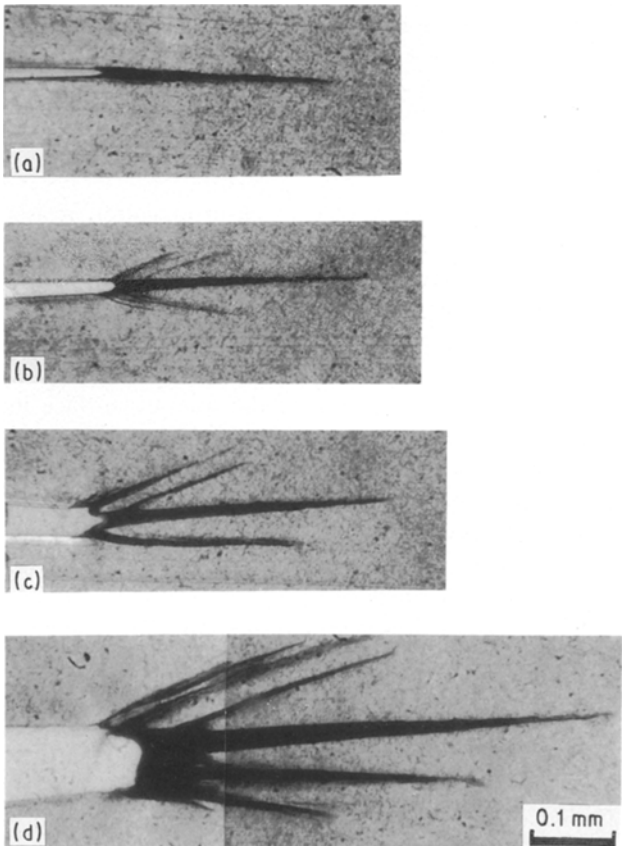

Figure 5 Transmission optical micrograph of thin sections prepared at the mid-plane of each specimen, showing the history of craze growth ahead of the notch. The number of fatigue cycles is indicated for each specimen. (a) First cycle, (b) 500 cycles, (c) 5000 cycles, (d) 70 000 cycles.

The specific nature of craze growth was noted to depend on the copolymer composition; nevertheless, the ultimate craze size at which crack initiation occurred was noted to display negligible dependence on the copolymer type. In our test configuration, the craze length associated with crack initiation was about 0.6 mm. The craze length after the first loading cycle as a function of the number of cycles for crack initiation in the three copolymers is shown in Fig. 7. Under identical loading conditions, it is shown that the length of the craze grown within the first loading cycle correlates directly with the number of cycles to initiation. The hexene copolymer has the longest craze and the shortest initiation time. The methylpentene copolymer has the shortest craze and exhibits the longest initiation time and the craze in the butene copolymer is of intermediate length and so is the

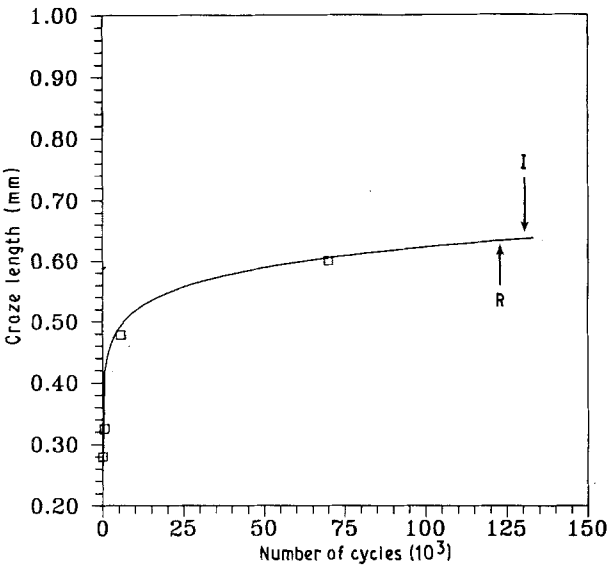

Figure 6 Measured craze length as a function of number of cycles. I and R, as in Fig. 4.

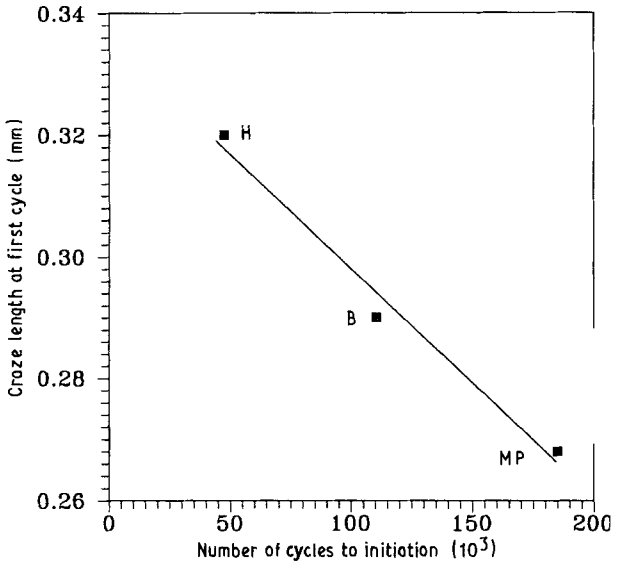

Figure 7 Measured craze length after the first loading cycle for the three copolymers versus the number of cycles to initiation. H, hexene; B, butene, MP, methyl–pentene copolymer.

initiation time. It has been noted earlier [1] that the resistance of these three copolymers to crack propagation is proportional to their resistance to crack initiation. If the craze length after one loading cycle (6 MPa) is considered indicative of the damage accumulation process, the data in Fig. 7 could bear interesting implications with regard to the chain microstructure which is beyond the scope of the present work. Subsequent analysis presents data on MP copolymer to explore kinetics of damage processes preceding crack initiation.

Fig. 8 exhibits typical rupture events within the front craze membrane. The dark regions are reflections of holes ruptured within the membrane. Smaller holes coalesce to develop larger ruptures. Microscopic observations of the specimens under load indicated that the front membrane ruptures appeared to have

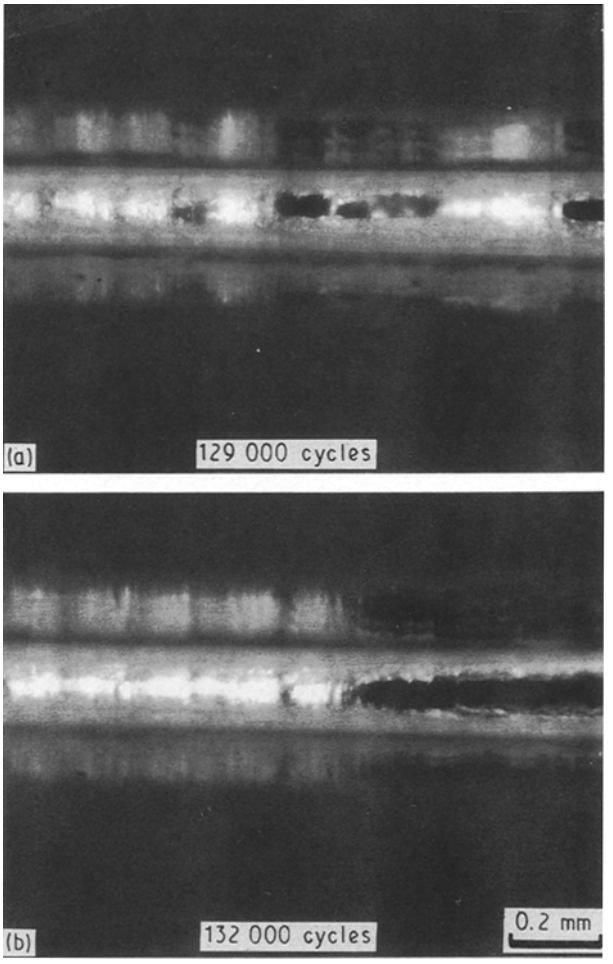

Figure 8 Microscopic view into the root of the notch showing typical rupture events within the front craze membrane. The dark regions are reflection of holes ruptured within the craze membrane. (a, b) Taken at the indicated number of cycles which fall between arrows R and I as shown in Fig. 4.

occurred into the depth of the entire craze. Fig. 8a and b are taken at a number of cycles which fall between arrows R and I in Fig. 4. This process continued with time until 90% of the membrane was ruptured. The other 10% (5% on each side) remained intact due to plane-stress effects. The membrane portion dominated by plane stress experienced less constraint and thus must have exhibited more plastic deformation. Fig. 9a and b show micrographs of thin sections prepared ahead of the front membrane, in a plane normal to the craze-propagation direction. The figure shows the extent of craze growth relative to the specimen edges. Fig. 9a shows that the edge of the root craze (vertical arrow marked Rc) is 20 μm away from the specimen edge. A similar view from a deeper section (Fig. 9b) shows the craze edge is displaced further from the edge of the specimen (0.5 mm). These and similar micrographs suggest that the outermost craze tip is semicircular. That is, the root craze appears to assume a penny-shaped configuration.

In accordance with the configuration assumed by the root craze, the crack-initiation process is concluded when the majority of the craze material has been ruptured to form a traction-free surface, i.e. a

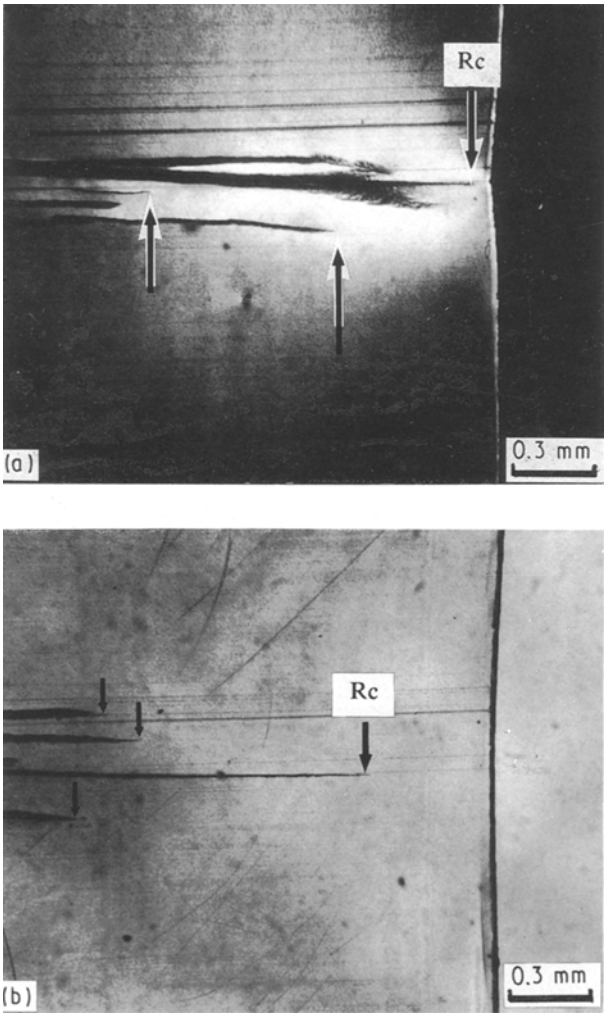

Figure 9 (a) Transmission micrograph of a thin section taken from a specimen interrupted before initiation. The photograph shows a region near a specimen edge ahead of the craze membrane in a plane normal to the crack propagation direction. Arrow Rc indicates the end of the root craze, and the other arrows indicate the end of side crazes. (b) Similar to (a) at a deeper section.

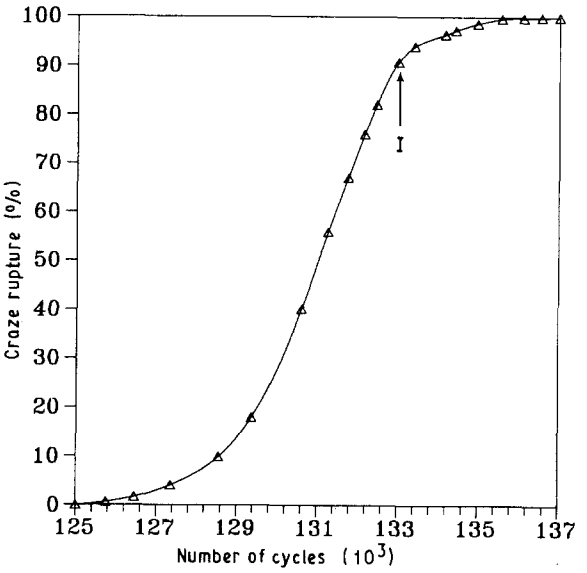

Figure 10 Craze rupture kinetics as a percentage of cumulative measured length of ruptured holes within the craze front normalized with respect to the total width (28 mm) as a function of the number of cycles. I, the designated point of initiation.

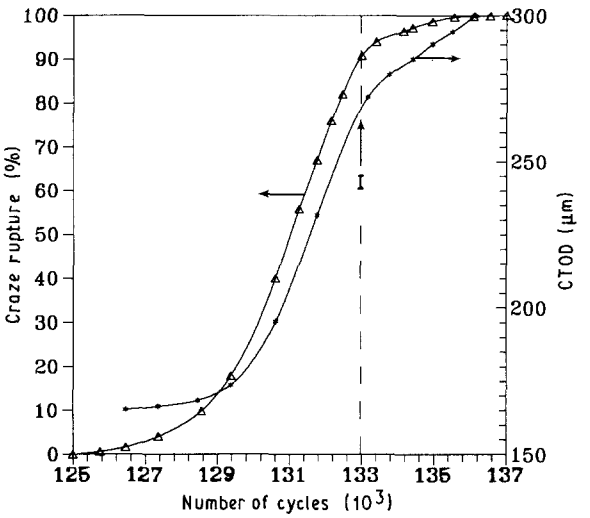

Figure 11 Superimposition of the craze-rupture kinetics in Fig. 10 over the kinetics of the CTOD within the box in Fig. 4. Horizontal arrows indicate the scale of each curve. Note an abrupt change in the slope of the two curves beyond the crack-initiation point (arrow I).

crack. This was achieved when about 90% of the front craze membrane was ruptured. The kinetics of this process is presented in Fig. 10 where the magnitude of craze rupture, expressed as the cumulative length of ruptured holes normalized with respect to the total membrane width (28 mm), is plotted as a function of the number of cycles. Only 10–20% of the craze damage was noted to have taken place within 50% of the time; the remaining damage, leading to crack initiation (arrow I), occurred subsequently. Additional membrane damage continues to occur even after crack initiation, but at a much slower rate. This delayed craze membrane damage occurred as the craze of the second crack band was being formed. This hypothesis may be supported by a superposition of the craze-rupture kinetics over the kinetics of the CTOD of Fig. 4 (box) as shown in Fig. 11. The congruence of the two phenomena is evident. An abrupt change in the slopes of the two curves beyond crack initiation (arrow I) suggests that the reduced rate of CTOD must have reflected stabilization of the craze zone configuration similar to that occurring prior to the onset of its steep rise at about 133 000 cycles. The latter observation suggests that the damage processes preceding crack propagation bear a strong similarity to those preceding crack initiation, an observation which reinforces the significance of this study.

4. Discussion

The experimental results described in the previous section, for the first time, present details on the kinetics of the plastic deformation at the crack tip and of the subsequent damage processes leading to crack initiation in MDPE pipe material. This procedure institutes an objective definition of crack initiation.

Although the study has been conducted on short-chain branched MDPE copolymers, its implications are equally applicable to other linear polymers because crack initiation inevitably ensues within the root craze whether the plastic zone comprises crazes or shear deformation. The results accomplished in the present inquiry also draw attention to distinct issues including applicability of plastic zone models, kinetics of craze evolution, distinction between craze growth and rupture of craze material leading to crack initiation. These points are discussed below.

4.1. Plastic-zone models

Plastic-zone models, namely Irwin's [22] and Dugdale/Barenblatt (D/B) [23, 24] are commonly used in fracture mechanics to calculate the extent of yielding at a notch tip due to external load. On the other hand, the Rice integral calculates the energy release associated with the crack tip and the affiliated plasticity. In our case, the D/B analysis is more relevant because the shape of the craze zone bears more resemblance to the plastic strip perceived by the D/B model. According to this model, the craze length, c, is given by

$$c = \frac{\pi}{8}\left[\frac{K_I f(a/b)}{\sigma_y}\right]^2 \quad (1)$$

where σ_y is the yield stress, K_I is the stress intensity factor for infinitely wide plate and $f(a/b)$ is the applicable geometric correction factor. An exact solution for the stress intensity factor of our specimen is not available. Owing to its acute departure from the conventional arc configuration [18], an effective value of stress intensity factor has been computed from a superposition of the normal and bending fields of single-edge notched configurations [25]. According to this approximation, $f(a/b)$ was found to be equal to 1.25 for our specimen.

The necking within the plastic strip (D/B zone) results in a finite displacement at its end approaching the crack tip, crack-tip opening displacement (CTOD), whose value, δ, is given by [26]

$$\delta = \frac{8\sigma_y a}{\pi E}\ln\left(\cos\frac{\pi\sigma}{2\sigma_y}\right)^{-1} \quad (2)$$

With decreasing σ/σ_y (and hence c/a) this will asymptotically approach

$$\delta = \frac{K_I^2}{E\sigma_y}(1-\nu^2) \quad (3)$$

The validity of the above relationships has been demonstrated analytically for small-scale yielding conditions for values of $\sigma/\sigma_y < 0.4$ [26]. This stress ratio in our case is 0.3. It should be also noted that these relationships employ one external parameter, K_I, thus their application necessitates that the crack-tip conditions be dominated by K_I, a criterion which appears to be satisfied by noting that the maximum size of the plastic zone is too considerably when compared to the ligament (7%) as deduced from Figs 4 and 6.

The D/B model as outlined above predicts a craze length $c = 0.81$ mm. Comparison with the fully developed craze size of 0.62 mm noted in Fig. 6 suggests that the D/B model gives rise to about 30% overestimate. On the other hand, the model yields a CTOD for our test conditions of $\delta = 0.075$ mm which is only half the experimentally observed value ($\delta = 0.150$ mm). The 30% departure of the D/B model in predicting the craze length is generally acceptable and perhaps originates from two sources. The first pertains to the crude nature of estimating the stress-intensity factor and the second relates to the specific nature of the yielding process taking place within the craze. The yield stress value employed in the model is taken as that determined from regular tensile-test specimens. The scale, the rate and the constraint under which yielding occurs within the craze is probably different from that prevailing in the bulk.

4.2. Craze kinetics

It is generally accepted that craze growth to a fully developed state precedes its breakdown to become a crack. In this regard, craze growth is a stable process that is driven by the energy available at its advancing tip and crack initiation is a manifestation of its instability. This instability is different from the crack instability in that as the craze becomes longer its speed diminishes (Fig. 6). A plot of the craze speed as a function of its lengths normalized to the specimen thickness is shown in Fig. 12. This behaviour is clearly opposite to that of normal crack-propagation behaviour under similar conditions.

The time-dependent craze length (Fig. 6) follows a simple power function of the form $c(t) = Ct^n$. The constant C and the power n are found to be 2.7×10^{-4} and 0.086, respectively. Similar measurements on other polymers [27, 28] suggest that the craze-growth exponent seemingly correlates with the ductility of the polymer. For example, the craze-growth exponents for PS, PMMA and PC are 0.150, 0.226 and 0.08. The observed exponential craze-growth behaviour was modelled by Argon and Salama [27] and earlier by Williams and Marshall [28]. The latter is of relevance in the present study. In their model, Williams and Marshall substituted the yield stress in the D/B model by a time-dependent function which leads to the following expression for the craze-growth rate

$$c(t) = \frac{\pi}{8}\frac{K_I^2}{(\varepsilon_y E_o)^2}t^n \quad (4)$$

where E_o is the initial value of the elastic modulus and ε_y is the strain at yield. This equation fits our data with a three-fold discrepancy in the $(\pi/8)\ (K_I/\varepsilon_y E_o)^2$ term which is acceptable in view of the nature of the underlying assumptions. It is a predicament, however, to perceive craze growth as being driven by a stress intensity factor. A more rational statement of Equation 4 may be reached by invoking a time-dependent energy release rate, i.e. $G_I(t) = G_I(0)\ t^n$ which replaces K^2/E in the D/B equation. This passageway to obtaining a time-dependent craze length from the D/B model

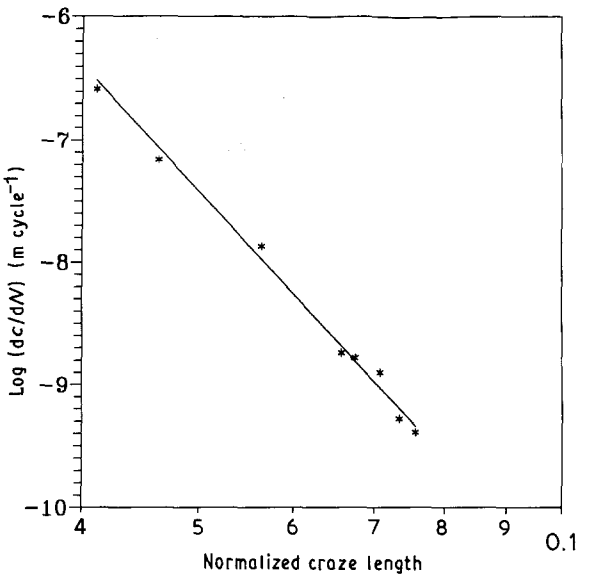

Figure 12 Logarithmic rate of craze growth as a function of craze length normalized to the total depth of the specimen.

is less cumbersome, particularly in view of the experimental evidence that the compliance, and therefore the potential energy, associated with craze growth exhibits a similar power character.

4.3. Damage of craze material

Crack advance in MDPE and many other linear polymers typically involves time-dependent craze growth *and* subsequent craze rupture to create traction-free crack "surfaces". It is the combination of these two processes which constitute the source of the resistance to crack propagation. Current literature does not usually resolve the two processes but consider them as one. Nonetheless, comparing the data in Figs 6 and 10, it is noted that the craze growth and rupture are seemingly distinct processes, each exhibiting its own functional character. Craze growth predominantly dominates the major segment of initiation lifetime. It was only after 125 000 cycles of craze-growth time (94% N_i) that the onset of craze rupture was noted. Thus, in this case the rupture of craze membranes leading to material separation (i.e. transforming the craze into a crack) represents only 6% of the initiation lifetime. Small as the contribution of craze rupture might appear, its significance lies in the notion that the resistance of a material to crazing might be different from its resistance to craze rupture. Judging from the evolution of the CTOD (Figs 4 and 5), and noting that CTOD is proportional to the energy release rate, it could be concluded that the majority of energy release is associated with craze rupture.

Finally, the dependence of the initial craze size and the number of cycles-to-initiation on the type of comonomer (Fig. 7) is of particular interest in probing the role of molecular processes to SCG resistance. If one argues that the tie molecules play a major role in the resistance to craze formation and rupture, therefore, it might be reasonable to perceive that the relative ease of the mobility of tie molecules is more effective in the following order of branch type: butyl (due to hexene comonomer), ethyl (due to butene comonomer) then isobutyl (due to methylpentene comonomer). The latter perhaps provides more efficient tie entanglements. Higher mobility of the tie chains facilitates initial and subsequent craze growth, leading to shorter lifetime.

5. Conclusion

The study presented above shows that the craze zone in MDPE copolymers grows to a fully developed configuration prior to crack initiation. Crack initiation occurs by rupture of the root craze membrane which occurs only at the final portion of the initiation lifetime after the craze has reached its fully developed configuration. The Dugdale/Barenblatt model for the plastic zone describes the craze length with acceptable accuracy, but departs significantly in predicting the crack-tip opening displacement due to multiple craze growth emanating from the notch tip. A time-dependent form of the D/B model describes the craze-growth kinetics.

Acknowledgements

The authors acknowledge the financial support of the Gas Research Institute, contract 5083-260-2031, and also thank Dr Max Klein for useful discussions and suggestions throughout the experiment and during preparation of the manuscript.

References

1. E. SHOWAIB, J. J. STREBEL and A. MOET, in "Proceedings of the Twelfth Plastic Fuel Gas Pipe Symposium", Boston, MA, September 1991, edited by L. C. Bradbury (American Gas Association, Arlington, VA, 1991) p. 427.
2. N. BROWN and X. LU, in "1989 GRI Annual Report 89/0169" (Gas Research Institute, Chicago, IL, February 1989) p. 47.
3. M. F. KANNINEN, P. E. O'DONOGHUE, C. H. POPELAR and V. H. KENNER, *Engng Fract. Mech.* **36** (1990) 903.
4. C. H. POPELAR, V. H. KENNER, S. F. POPELAR and M. C. PFEIL, in "Proceedings of the Twelfth Plastic Fuel Gas Pipe Symposium", Boston, MA, September 1991, edited by L. C. Bradbury (American Gas Association, Arlington, VA, 1991) p. 372.
5. M.-R. LIN, M. E. FINE and T. MURA, *Acta Metall.* **34** (1986) 619.
6. T. MURA and Y. NAKASONE, *J. Appl. Mech.* **57** (1990) 408.
7. G. GLINKA, *Engng Fract. Mech.* **5** (1986) 939.
8. A. NEWPORT and G. GLINKA, *Exp. Mech.* **30** (1990) 208.
9. T. H. TOPPER, R. M. WETZEL and J. MORROW, *J. Mater.* **4** (1969) 200.
10. Y. FURUYA and H. SHIMADA, *Engng Fract. Mech.* **23** (1986) 983.
11. A. SHIMAMOTO, S. TAKAHASHI and A. YOKOTA, *Exp. Mech.* **31** (1991) 65.
12. X. LU and N. BROWN, *J. Mater. Sci.* **21** (1986) 2423.
13. N. BROWN and S. K. BHATTACHARYA, *ibid.* **20** (1985) 4553.
14. A. LUSTIGER and R. D. CORNELIUSSEN, *ibid.* **22** (1987) 2470.
15. K. CHAOUI, PhD thesis, Case Western Reserve University (1989) 58.
16. H. NISHIMURA, T. SHISHIDO, M. NAKAHURA, H. SHIBANO and K. KITAO, *J. Jpn Soc. Process. Plastics Seikeikako* **1** (1989) 318.

17. H. NISHIMURA and M. NAKAHURA, private communication (1989).
18. Annual Book of ASTM Standards 202 (American Society for Testing and Materials, Philadelphia, PA, 1988) p. E399-83.
19. X. LU, R. QIAN and N. BROWN, *J. Mater. Sci.* **26** (1991) 881.
20. A. LUSTIGER, M. J. CASSADY, F. S. URALIL and L. E. HULBERT, "Field Failure Reference Catalog for Polyethylene Gas Piping" (Gas Research Institute, Chicago, IL, 1986) p. 34.
21. J. J. STREBEL and A. MOET, *J. Mater. Sci.* **26** (1991) 5671.
22. D. BROEK, in "Elementary Engineering Fracture Mechanics" (Martinus Nijhoff, Dordrecht, Boston, Lancaster, 1987) p. 100.
23. D. S. DUGDALE, *J. Mech. Phys. Solids* **8** (1960) 100.
24. G. I. BARENBLATT, *Adv. Appl. Mech.* **7** (1962) 55.
25. H. TADA, C. PARIS and R. IRWIN, in "The Stress Analysis of Cracks Handbook" (Paris Productions, 1985, MO, USA) pp. 2–10.
26. K. HELLAN, in "Introduction to Fracture Mechanics" (McGraw-Hill, New York, 1984) p. 21.
27. A. S. ARGON and M. M. SALAMA, *Phil. Mag.* **36** (1977) 1217.
28. J. G. WILLIAM and G. P. MARSHALL, *Proc. R. Soc. Lond.* **A342** (1975) 55.

Received 12 October
and accepted 19 November 1992